# Efficient Room-Temperature Continuous-Wave AlGaInP/AlGaAs Visible (670 nm) Vertical-Cavity Surface-Emitting Laser Diodes

R. P. Schneider, Jr., K. D. Choquette, J. A. Lott, K. L. Lear, Member, IEEE, J. J. Figiel and K. J. Malloy, Member, IEEE

*Abstract*— Significant improvement in the performance of AlGaInP/AlGaAs visible vertical-cavity surface-emitting laser diodes has been achieved in gain-guided planar-geometry devices utilizing proton implants to define the current injection path. Threshold currents as low as 1.25 mA were measured on 10 $\mu$m-diameter devices, with maximum power output of 0.33 mW from larger devices. Continuous-wave (cw) lasing was achieved at temperatures as high as 45°C. The improved diode performance is attributed to better lateral heat-sinking and reduced parasitic heat generation afforded by the planar device structure, relative to previously-reported air-post structures. This work represents the first realization of efficient room-temperature operation of AlGaInP-based visible VCSEL diodes.

## I. INTRODUCTION

VISIBLE vertical-cavity surface-emitting laser diodes (VCSELs) have the potential to fufill many critical optoelectronic application areas, including scanning, printing, plastic fiber-based optical communications sources, and display. Recently electrically-injected lasing, at room-temperature and under pulsed excitation, was demonstrated in an AlGaInP/AlGaAs visible ($\lambda \sim 650$) nm VCSEL diode [1] employing an extended optical cavity for efficient electrical injection [2]. These initial devices operated inefficiently, in part due to insufficient gain available to offset losses [3]. Indeed, it was found that by increasing the available gain and decreasing the free-carrier absorption losses room-temperature continuous-wave (cw) operation could be achieved without extensive modification to the epitaxial layer structure [4]. However power output in these devices remained very low ($\sim$25 $\mu$W from a 20 $\mu$m-diameter etched "air-post"), due in part to the etched-post device geometry which provides less efficient heat-sinking than the more conventional planar proton-implanted VCSEL diode geometry typically employed with near-IR VCSELs [5].

In the present Letter we report significantly improved visible ($\lambda \sim 670$) nm VCSEL diode performance in gain-guided planar-geometry devices utilizing proton implants to define the current injection path. Using an epitaxial layer structure similar

to previous cw devices, we have now achieved threshold currents as low as 1.25 mA from a 10 $\mu$m device, with power outputs as high as 0.33 mW from larger devices. Furthermore, cw lasing is achieved at temperatures as high as 45°C. The improved diode performance is attributed to better heat-sinking, as well as reduced parasitic heat generation, afforded by the planar device structure.

## II. DEVICE DESIGN, GROWTH AND FABRICATION

A real-space energy-band schematic of the epitaxial layer design is shown in Fig. 1a. The entire structure is grown using low-pressure metalorganic vapor-phase epitaxy (MOVPE) on $n+$ GaAs substrates misoriented 6° off the (100) towards the nearest $\langle 111 \rangle A$. Growth conditions are described in greater detail elsewhere [6], [7]. The DBRs are composed of 0.15$\lambda$ layers of AlAs and Al$_{0.5}$Ga$_{0.5}$As separated by 0.1$\lambda$-thick segments continuously graded in a psuedo-parabolic composition profile. The graded portion is included to flatten out heterojunction barrier "spikes" in the conduction and valence bands resulting from the composition discontinuity, to reduce series resistance in the DBRs and allow reduced doping. Similar approaches in MBE-grown 980 nm VCSELs have recently resulted in record efficiencies [8]. The $n$-DBR is doped with Si to $n \sim 2 \times 10^{18}$ cm$^{-3}$, while the average hole concentration in the $C$-doped $p$-DBR is $p \sim 2 \times 10^{18}$ cm$^{-3}$, with $p \sim 5 - 10 \times 10^{17}$ cm$^{-3}$ in the first 5 DBR pair nearest the cavity to reduce free-carrier absorption losses. A 10 nm-thick $p$++ GaAs contact layer and the top 2 DBR pair are doped to $p \sim 0.5 - 2 \times 10^{20}$/cm$^{-3}$ to reduce contact resistance and lateral spreading resistance. 55.5 DBR pair are used for the high reflector, with 36 pair for the output coupler. The calculated peak reflectance for the latter DBR is 99.93%, taking into account the pseudo-parabolic grade. The very high reflectivity is designed to yield low lasing thresholds, however at some cost in output power.

The optical cavity consists of a central 2$\lambda$ undoped active portion, surrounded by $n$- and $p$-type 3$\lambda$-thick Al$_{0.5}$In$_{0.5}$P spacer layers. The spacers are doped with Si and Mg to $n \sim 1 \times 10^{18}$ cm$^{-3}$ and $p \sim 7 \times 10^{17}$ cm$^{-3}$, respectively, and are included to improve carrier injection efficiency [2]. The active region is comprised of 3 Ga$_{1-x}$In$_x$P strained quantum wells (QWs) separated by 6 nm-thick (Al$_{0.5}$Ga$_{0.5}$)$_{0.5}$In$_{0.5}$P barriers. In two different wafers the QW compositions and thicknesses are ($L_W \sim 8$ nm, $x \sim 0.54$) and ($L_W \sim 6$ nm, $x \sim 0.57$),
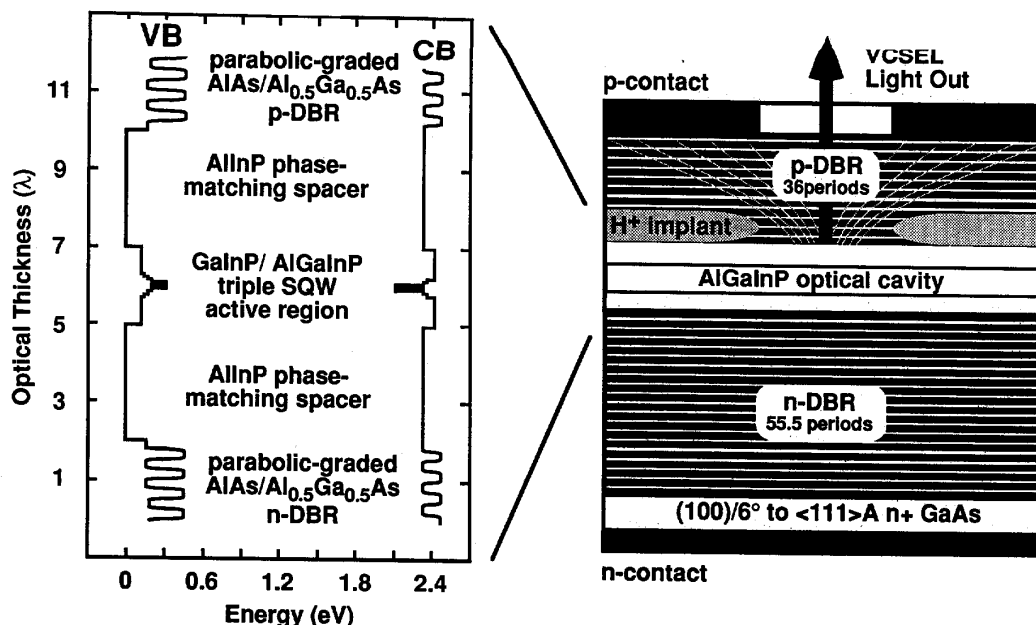
Fig. 1. Schematic diagram of (a) the visible VCSEL epitaxial layer structure, including the 8λ-thick AlGaInP active optical cavity and several pseudo-parabolically graded DBR pair on either side of the cavity, and (b) the visible VCSEL device geometry, including proton implant for device isolation and current funneling.

respectively. The compositions were adjusted to yield similar emission wavelength (photoluminescence calibration of $\lambda \sim$ 663–665 nm), and thus similar total confinement potentials, despite the varying QW thickness. The QW active region is surrounded by an $(Al_y Ga_{1-y})_{0.5} In_{0.5}P$ step-graded barrier, with $y$ increasing from ~0.5 to ~0.65 in 4 20 nm-thick steps. The remainder of the central 2λ portion of the optical cavity consists of undoped $(Al_{0.7}Ga_{0.3})_{0.5}In_{0.5}P$. The active region was carefully optimized using conventional single-QW edge-emitting laser diodes with $Al_{0.5}In_{0.5}P$ cladding layers, for which state of the art performance, including threshold current densities of 200–300 A/cm² and a characteristic temperature of $T_0 = 156$ K at $\lambda = 680$ nm, was obtained [9]. The very high $T_0$ indicates relatively low thermal leakage in these heterostructures. This property is particularly critical for visible VCSEL design, as visible laser diodes are known to be subject to carrier leakage resulting from relatively poor confinement [10], and even IR VCSELs are subject to significant carrier leakage due to excessive heating and high current densities [11].

A schematic of the as-fabricated device geometry is given in Fig. 1b. The devices were fabricated using a double $H^+$ implant for lateral current confinement and device isolation. The implants were performed at 410 keV, with a dose of $4 \times 10^{14}$ cm$^{-2}$, and 370 keV, with a dose of $1 \times 10^{14}$/cm$^{-2}$. The implants are designed to center the peak of the damage at the optical cavity-DBR junction and funnel hole current

above the cavity-DBR junction. Little lateral current spreading is anticipated in the upper 3λ spacer layer because of the relatively high resistivity of $p$-type $Al_{0.5}In_{0.5}P$. The implant defines apertures of 10–25 μm, and optical apertures in the $p$-contact metal are 10–35 μm in diameter. After implant a $125 \times 75$ μm mesa is defined by plasma etching through the $p$-DBR to the top of the optical cavity.

## III. DEVICE PERFORMANCE

Devices were tested in the temperature range 22°C (room-temperature) to 50°C under cw excitation. Shown in Fig. 2 are representative light vs. current (L-I) and current vs. voltage (I-V) characteristics for devices operating at room temperature at a wavelength of ~670 nm. It should be noted that separate analysis of these wafers has indicated that the cavity resonance is blue-shifted with respect to the peak of the gain at operational temperatures [12]. Threshold currents $I_{TH}$ as low as 1.25 mA were observed for 10 μm devices at 670 nm. Threshold current density as low as ~1000 A/cm² was also observed for these triple QW devices, only 3–5 times that of our single QW edge-emitting lasers. The very high output coupler reflectivity is at least partly responsible for the low thresholds. Nevertheless, output powers as high as 0.33 mW were measured for devices $\leq$ 25 μm in diameter. The voltage at threshold $V_{TH}$ is typically 2.5–3.0 V. Kinks in the L-I characteristics are due to the occurence of higher-order transverse modes, a behavior typical of gain-guided VCSELs
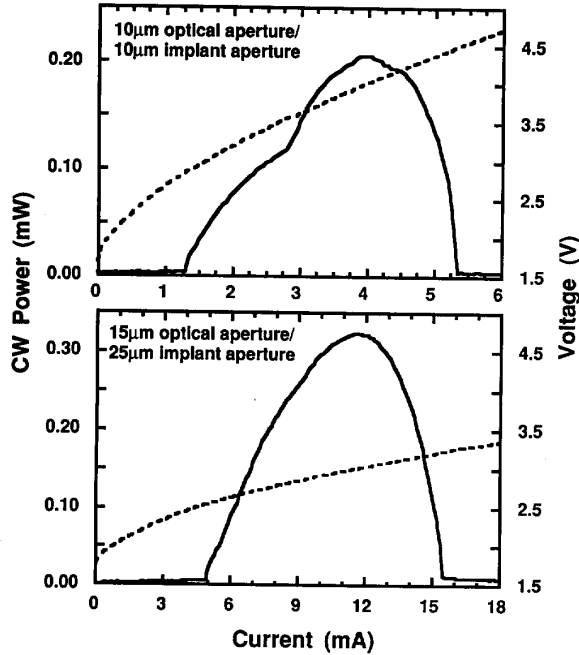
Fig. 2. Room-temperature CW light-current (L-I) and current-voltage (I-V) plots for representative visible VCSELs. Data are shown for devices with (a) 10 $\mu$m implant and 10 $\mu$m optical (contact) apertures, and (b) 25 $\mu$m implant aperture and 15 $\mu$m optical apertures. Thresholds as low as 1.25 mA and power output as high as 0.33 mW are indicated in the figures.
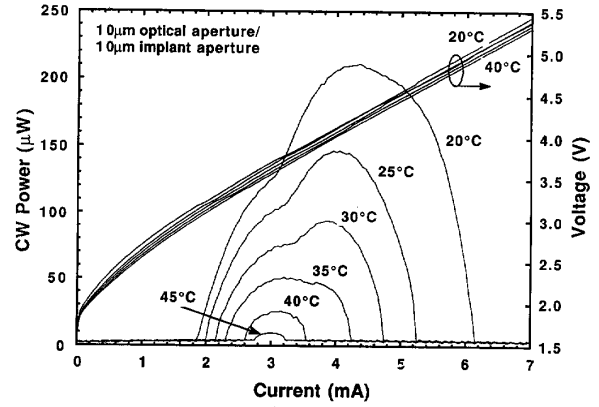


Fig. 3. CW light-current (L-I) and current-voltage (I-V) traces for a representative visible VCSEL diode at varying heat-sink temperatures between room temperature and 45°C. CW lasing is achieved at temperatures as high as 45°C, even though the optimal cavity resonance-QW gain overlap occurs below room temperature. Kinks in the L-I characteristics are due to the occurence of higher-order transverse modes, a behavior typical of gain-guided VCSELs [13].

[13]. We have observed that devices with implant apertures smaller than their contact apertures also exhibit cw operation, indicating very low lateral resistance in the upper $p$-DBR. Similar characteristics are observed from devices fabricated on each of the two wafers.

L-I characteristics for a 10 $\mu$m device tested at varying heat-sink temperatures is given in Fig. 3. CW lasing is achieved for heat-sink temperatures as high as 45°C. Because the temperature-dependent properties of VCSELs are dominated by the temperature-dependent overlap between the cavity resonance and the peak of the gain [14], these data are not representative of the fundamental limits imposed by the material and device geometry.

Further performance enhancements can be anticipated through additional design refinements, including red-shifting the cavity resonance with respect to the peak of the gain [15], reduction of the reflectivity of the output-coupling DBR for increased external efficiency [16] and further refinement of the doping and grading schemes in the DBRs. Finally, the extended-cavity design used here provides efficient electrical injection between the DBRs and the optical cavity, and device performance achieved with this approach significantly exceeds that obtained with more conventional short ($1\lambda$) cavity designs [17]. However, modification to the doping and interface growth schemes to allow efficient injection with a short cavity should yield a corresponding reduction in cavity losses, more efficient lateral current confinement, and improved temperature characteristics (due to the low thermal impedance associated with AlGaAs relative to the AlGaInP alloys).

## IV. SUMMARY AND CONCLUSION

Significant improvement in the room-temperature cw performance of AlGaInP/AlGaAs visible vertical-cavity surface-emitting laser diodes has been achieved in gain-guided planar-geometry devices defined by proton implantation. Threshold currents as low as 1.25 mA were measured in 10 $\mu$m-diameter devices, with maximum power output of 0.33 mW from devices with apertures $\leq$25 $\mu$m. CW lasing was achieved at temperatures as high as 45°C. The improved diode performance is attributed to the superior heat-sinking and reduced parasitic heat generation afforded by the planar device geometry, relative to previous air-post device geometries. These results establish useful performance levels in AlGaInP-based visible VCSEL diodes, and open the door for their use in a variety of applications requiring visible laser light sources. For example, recent tests of these devices indicate that they are particularly well-suited for insertion in fiber-based data communication links [18].

## REFERENCES

[1] J. A. Lott and R. P. Schneider, "Electrically-injected visible (639–661 nm) vertical cavity surface emitting lasers" Electron. Lett., vol. 29, pp. 830–832, 1993.

[2] R. P. Schneider, Jr. and J. A. Lott, "Cavity design for improved electrical injection in AlGaInP/AlGaAs visible vertical cavity surface-emitting laser diodes," Appl. Phys. Lett., vol. 63, pp. 917–919, 1993.

[3] J. A. Lott, R. P. Schneider, Jr., J. C. Zolper and K. J. Malloy, "AlGaInP visible vertical-cavity surface-emitting lasers operating with

gain contributions from the $n = 2$ quantum well transition," *Appl. Phys. Lett.*, submitted for publication.

[4] J. A. Lott, R. P. Schneider, Jr., K. D. Choquette, S. P. Kilcoyne and J. J. Figiel, "Room-temperature continuous-wave operation of red vertical cavity surface-emitting laser diodes," *Electron. Lett.*, submitted for publication.

[5] See, for example, *J. Quantum Electron.*, vol. 27, pp. 1332–1425, 1991.

[6] R. P. Schneider, Jr., E. D. Jones, J. A. Lott and R. P. Bryan, "Photoluminescence linewidths in ordered and disordered InAlGaP alloys grown by metalorganic vapor phase epitaxy," *J. Appl. Phys.*, vol. 72, p. 5397, 1992..

[7] R. P. Schneider, Jr., R. P. Bryan, J. A. Lott, E. D. Jones and G. R. Olbright, "MOVPE growth of InAlGaP-based visible vertical-cavity surface-emitting lasers," *J. Cryst. Growth*, vol. 124, p. 763, 1992.

[8] K. L. Lear and S. A. Chalmers, "High single-mode power conversion efficiency vertical-cavity top-surace-emitting lasers," *Photon. Technol. Lett.*, vol. 5, pp. 972–975, 1993.

[9] R. P. Schneider, Jr., K. L. Lear and J. A. Lott, unpublished.

[10] D. P. Bour, D. W. Treat, R. L. Thornton, R. S. Geels and D. F. Welch, "Drift leakage current in AlGaInP quantum well lasers," *IEEE J. Quantum Electron.*, vol. 29, p. 1337, 1993..

[11] J. W. Scott, S. W. Corzine, D. B. Young and L. A. Coldren, "Mod-

eling the current to light characteristics of index-guided vertical-cavity surface-emitting lasers," *Appl. Phys. Lett.*, vol. 62, p. 1050, 1993.

[12] K. D. Choquette, R. P. Schneider, Jr. and J. A. Lott, unpublished.

[13] K. Tai, Y. Lai, K. F. Huang, T. C. Huamg, T. D. Lee and C. C. Wu, "Transverse mode emission characteristics of gain-guided surface emitting lasers," *Appl. Phys. Lett.*, vol. 63, pp. 2624–2626, 1993.

[14] G. Hasnain, K. Tai, L. Yang, Y. H. Wang, R. J. Fischer, J. D. Wynn, B. Weir, N. K. Dutta and A. Y. Cho, "Performance of gain-guided surface-emitting lasers with semiconductor distributed Bragg reflectors," *J. Quantum Electron.*, vol. 27, pp. 1377–1385, 1991.

[15] D. B. Young, J. W. Scott, F. H. Peters, B. J. Thibeault, S. W. Corzine, M. G. Peters, S.-L. Lee and L. A. Coldren, "High-power temperature-insensitive gain-offset InGaAs/GaAs vertical-cavity surface-emitting lasers," *Photon. Technol. Lett.*, vol. 5, pp. 129–132, 1993.

[16] R. S. Geels, S. W. Corzine and L. A. Coldren, "InGaAs vertical-cavity surface-emitting lasers," *J. Quantum Electron.*, vol. 27, pp. 1359–1367, 1991.

[17] K. F. Huang, K. Tai, C. C. Wu and J. D. Wynn, "Continuous-wave visible InGaP/InGaAlP quantum well surface-emitting laser diodes," *Electron. Lett.*, vol. 29, p. 1314, 1993.

[18] D. M. Kuchta, F. J. Canora, R. P. Schneider, Jr., J. A. Lott and K. D. Choquette, unpublished.